





Anaerobic methane oxidation is an important sink for methane in the ocean's largest oxygen minimum zone

Bo Thamdrup ^{1,*} Herdís G. R. Steinsdóttir ¹ Anthony D. Bertagnolli,² Cory C. Padilla,² Nastassia V. Patin,² Emilio Garcia-Robledo ^{3,4} Laura A. Bristow ¹ Frank J. Stewart²

¹Department of Biology, University of Southern Denmark, Odense M, Denmark

²School of Biological Sciences, Georgia Institute of Technology, Atlanta, Georgia

³Department of Biology, University of Cadiz, Cadiz, Spain

⁴Centre for Water Technology, Aarhus University, Aarhus, Denmark

Abstract

We investigated methane oxidation in the oxygen minimum zone (OMZ) of the eastern tropical North Pacific (ETNP) off central Mexico. Methane concentrations in the anoxic core of the OMZ reached ~ 20 nmol L⁻¹ at off shelf sites and 34 nmol L⁻¹ at a shelf site. Rates of methane oxidation were determined in ship-board incubations with ³H-labeled methane at O₂ concentrations 0–75 nmol L⁻¹. In vertical profiles at off-shelf stations, highest rates were found between the secondary nitrite maximum at ~ 130 m and the methane maximum at 300–400 m in the anoxic core. Methane oxidation was inhibited by addition of 1 μmol L⁻¹ oxygen, which, together with the depth distribution, indicated an anaerobic pathway. A coupling to nitrite reduction was further indicated by the inhibitory effect of the nitric oxide scavenger 2-phenyl-4,4,5,5-tetramethylimidazole-1-oxyl-3-oxide (PTIO). Metatranscriptomes from the anoxic OMZ core supported the likely involvement of nitrite-reducing bacteria of the NC10 clade in anaerobic methane oxidation, but also indicated a potential role for nitrate-reducing euryarchaeotal methane oxidizers (ANME-2d). Gammaproteobacteria of the Methanococcales were further detected in both 16S rRNA gene amplicons and metatranscriptomes, but the role of these presumed obligately aerobic methane oxidizers in the anoxic OMZ core is unclear. Given available estimates of water residence time, the measured rates and rate constants (up to ~ 1 yr⁻¹) imply that anaerobic methane oxidation is a substantial methane sink in the ETNP OMZ and hence attenuates the emission of methane from this and possibly other OMZs.

Oceanic oxygen minimum zones (OMZs) are pelagic waters with low oxygen concentrations. The largest OMZs are found in the eastern tropical Pacific and the Arabian Sea where oxygen in the OMZ core is depleted to anoxia (Thamdrup et al. 2012; Tiano et al. 2014) and anaerobic metabolisms prevail. OMZs are intensely studied for their role in the marine nitrogen cycle, with about one-third of the removal of reactive nitrogen occurring there through microbial denitrification and anammox. Another potentially important but less explored biogeochemical aspect of OMZs is their role in methane cycling. The world's largest OMZ (Paulmier and Ruiz-Pino 2009), in the eastern tropical North Pacific (ETNP), is reported to contain the largest open-ocean accumulation of methane, estimated to 0.3 Tg (Sansone et al. 2001). The highest methane concentrations (10–100 nmol L⁻¹) occur in the anoxic OMZ core, but elevated levels can reach into the mixed layer (Sansone et al. 2001; Pack et al. 2015; Chronopoulou et al. 2017), and the upwelling areas with which the OMZs are associated are hotspots of marine methane emission

(Owens et al. 1991; Naqvi et al. 2010). Benthic methanogenesis is suggested to be a major source of methane in the ETNP OMZ (Sansone et al. 2001; Chronopoulou et al. 2017), yet high methane concentrations reach from hundreds to more than 1000 km away from the zone of contact between sediment and the anoxic OMZ core (Burke et al. 1983; Sansone et al. 2001; Pack et al. 2015; Fig. 1). It remains to be explored whether the distribution of methane in the OMZ merely reflects advection and lack of consumption, or whether other sources contribute (e.g., methanogenesis in the water column; Reeburgh 2007; Padilla et al. 2016). Likewise, it is not known whether anaerobic methane oxidation actively attenuates the accumulation of methane and its transfer to surface waters, thereby ultimately influencing the methane emissions in the OMZ regions.

Methane oxidation in the ETNP OMZ is indicated by increasing δ¹³C values offshore (Sansone et al. 2001) and has been quantified experimentally in OMZ waters (Pack et al. 2015; Chronopoulou et al. 2017). However, previous experimental studies did not take special measures to prevent the contamination with small amounts of oxygen, which is typically associated with sampling and shipboard incubations (De Brabandere

*Correspondence: bot@biology.sdu.dk

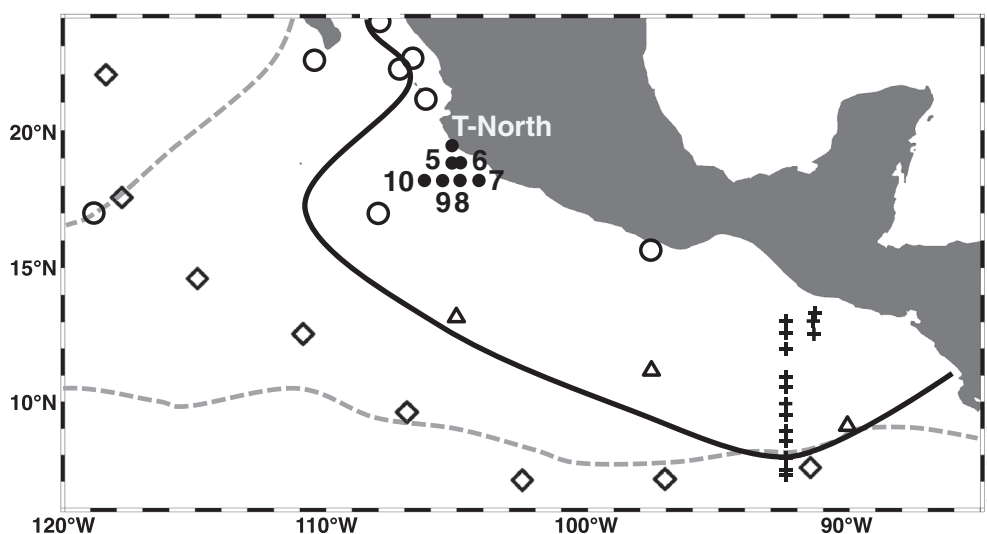


Fig. 1. Map of the ETNP OMZ with sampling positions from this study (filled circles) as well as from previous studies measuring the vertical methane distribution through the OMZ. Diamonds: Burke et al. (1983); open circles: Sansone et al. (2001, 2004); triangles: Pack et al. (2015); crosses: Chronopoulou et al. (2017). Stippled lines represent the northern and southern isopleth for an oxygen concentration of $9 \mu\text{mol L}^{-1}$ at 400 m depth (Sansone et al. 2001). The black curve encloses all stations with $\geq 10 \text{ nmol L}^{-1}$ methane at oxygen-depleted depths.

et al. 2012; Ganesh et al. 2015). Thus, it is not clear if the observed methane oxidation was anaerobic, as would necessarily be the case in the anoxic OMZ core. The first evidence of anaerobic methane oxidation in the ETNP OMZ was the discovery of a population of bacteria closely related to “*Candidatus Methyloirabilis oxyfera*” of the NC10 clade inhabiting the anoxic core (Padilla et al. 2016). The candidate genus *Methyloirabilis* contains obligately anaerobic methane oxidizers that use nitrite as an electron acceptor and appear to oxidize methane with molecular oxygen produced through the dismutation of nitric oxide (Ettwig et al. 2010). This reaction is thought to be catalyzed by a quinol-oxidizing nitric oxide reductase-like enzyme, qNor. In the ETNP, these organisms peaked in abundance at depths between the nitrite and methane maxima and were metabolically active as indicated by their transcription of several genes that encode enzymes of the suggested core metabolism (Padilla et al. 2016). Putative nitrite-dependent methane oxidizers of the NC10 clade have now been identified both in the northern and southern part of the ETNP OMZ (Padilla et al. 2016; Chronopoulou et al. 2017), and they were further indicated from NC10-like qNor-encoding transcripts in transcriptomes from the eastern tropical South Pacific OMZ (Dalsgaard et al. 2014; Ganesh et al. 2014).

Methanotrophs of the gammaproteobacterial order Methylococcales, typically known as aerobic methane oxidizers, have also been found in OMZ waters (Tavormina et al. 2013; Padilla et al. 2017). Members of this clade are able to perform partial denitrification to NO or N₂O (Kits et al. 2015; Padilla et al. 2017), and to oxidize methanol anaerobically (Dam et al. 2013), but anaerobic methane oxidation has not been demonstrated. Indeed, these microbes have typically been linked to OMZ boundaries, where

low or sporadic oxygen may be available for methane oxidation by particulate methane monooxygenases (PMOs) (Tavormina et al. 2013; Padilla et al. 2017), and they were not detected in the anoxic core of the ETNP OMZ in a previous study (Padilla et al. 2016). Other known anaerobic methanotrophs that couple methane oxidation to nitrate or sulfate reduction (Knittel and Boetius 2009; Haroon et al. 2013), such as “*Ca. Methanoperedens nitroreducens*” of the nitrate-reducing ANME-2d clade (Haroon et al. 2013), have not been reported from OMZ waters.

In order to explore the importance of anaerobic methane oxidation in OMZs and the potential implications of this process for the methane budgets of these biogeochemical hotspots, we quantified rates of methane oxidation in the anoxic core of the ETNP OMZ experimentally. We further evaluated the oxygen sensitivity and pathways of the process by manipulation of oxygen concentrations and addition of inhibitors, and we sought to identify the microbes that catalyze the process. We found (1) that methane is oxidized anaerobically with nitrate or nitrite as the likely terminal electron acceptor, (2) that affiliates of *Methyloirabilis* sp. likely contribute to the process, (3) that other nitrate-reducing or denitrifying microbes, including gammaproteobacterial methanotrophs, may also be involved, and (4) that anaerobic methane oxidation is a major sink in the methane budget of the OMZ.

Methods

Sites and chemical analyses

The OMZ of the ETNP was sampled off Manzanillo, Mexico in May 2017 from R/V *Oceanus* (cruise # OC1705; Fig. 1). Positions and types of samples collected at each station are listed in Table 1 with station numbers adopted from Padilla et al.

Table 1. Sampling positions and types of data collected at each station.

Station	Position	Types of data
5	18°55.3'N 105°12.6'W	Geochemistry, CH ₄ oxidation rates
6	18°54.0'N 104°54.0'W	Geochemistry, CH ₄ oxidation rates
7	18°12.0'N 104°12.1'W	Geochemistry
8	18°11.9'N 104°54.8'W	Geochemistry, CH ₄ oxidation rates
9	18°12.0'N 105°12.0'W	Geochemistry
10	18°12.0'N 106°17.8'W	Geochemistry, CH ₄ oxidation rates, DNA/RNA
T-North	19°30.0'N 105°12.6'W	Geochemistry, CH ₄ oxidation rates, DNA/RNA

Geochemical data include oxygen, methane, nitrite, and ammonium profiles; DNA and RNA analyses include 16S rRNA gene amplicon and non-rRNA transcriptomic sequences. See the text for different types of methane oxidation rate measurements made at each station.

(2016) and Garcia-Robledo et al. (2017). Oceanographic parameters were recorded with a Seabird SBE911 conductivity, temperature and depth-measuring device (CTD) equipped with a SBE43 oxygen sensor. High sensitivity oxygen measurements were further recorded with a STOX oxygen sensor interfaced with the CTD (Revsbech et al. 2009). Water samples were collected in 10-liter Niskin bottles on a CTD rosette and used for measurement of methane, nitrite, and ammonium concentrations as well as for incubations. Water for methane analysis was sampled through gas-tight Viton tubing into 50 mL serum bottles filled with three volumes overflow. The bottles were crimp-sealed with butyl rubber injection septa (La-Pha-Pack, GmbH) after introduction of a 2.5 mL headspace and addition of 100 μL 6 mol L⁻¹ HCl for preservation. Samples for nitrite were filtered (0.45 μm nylon) and analyzed on board, while samples for ammonium were immediately amended with orthophthaldehyde reagent (Holmes et al. 1999). Methane was quantified through headspace analysis using a gas chromatograph with a flame ionization detector (Thermo) and the concentration was calculated using the temperature- and salinity-dependent distribution coefficient (Wiesenburg and Guinasso 1979). Nitrite was analyzed spectrophotometrically (Grasshoff 1983) and ammonium was analyzed fluorometrically (Holmes et al. 1999).

Sampling and setup of incubations

Methane oxidation rates were measured in incubations with ³H-labeled methane (Valentine et al. 2001; Bussmann et al. 2015) using procedures developed for studies of anaerobic nitrogen cycling in OMZs with the aim of minimizing the effect of the oxygen contamination, which is so far inevitable during sampling and handling of OMZ waters (De Brabandere et al. 2014; Ganesh et al. 2015). Rate profiles were measured at one nearshore station over the shelf (T-North) and two off-shelf stations (8 and 10) along an inshore offshore transect, while various manipulatory experiments, described below,

were conducted at two stations each, differing in distance to the coast, and at two or three depths per station, with depths chosen to represent distinctive features in the geochemical zonation (see “Results” section).

For all experiments, water was sampled from 10-liter Niskin bottles through Viton tubing into 0.25-liter (rate profiles) or 1-liter (other types of experiments) glass bottles allowing ≥ 2 volumes overflow. The bottles were sealed with deoxygenated (≥ 1 month in He atmosphere) butyl rubber stoppers without bubbles and immediately brought to a thermostated laboratory (15°C) where a headspace was introduced and the water was purged with N₂ through a glass frit for 10 min to remove the small amounts of oxygen introduced during sampling. The water was decanted through glass and Viton tubing into 12 mL Exetainers (Labco) that were filled with overflow and sealed with deoxygenated chlorobutyl rubber septa. A 1 mL N₂ headspace was then introduced through the septum and subsequently flushed twice after 30 s of shaking to drive traces of oxygen out of the water. For manipulation experiments, inhibitors, ammonium, and dithionite were injected before flushing the headspace. Oxygen concentrations in the flushed Exetainers were ≤ 75 nmol L⁻¹ as determined with optode spots (see “Oxygen sensitivity experiments” section). The samples were then injected with 10 μL gaseous ¹H/³H-methane/N₂ mixture (~ 5 kBq μL^{-1} , details below), and incubation commenced in a dark incubator kept near in situ temperature (14°C). Activity was terminated by injection of 100 μL 50% (w/v) zinc chloride into three parallel vials per time point. The first set of vials was fixed immediately after injection of the tracer and thus served as killed controls accounting for abiotic decomposition of the tracer. The standard incubation time was 24 h except for the time series and inhibitor experiments for which incubation times varied between 6 and 96 h to check for linearity during the first 24 h used for standard incubations and reveal potential time dependence of inhibitor effects.

Addition of labeled and unlabeled methane

The gaseous tracer mixture was made up during the cruise from 37 MBq aliquots of ³H-CH₄ (single-labeled, 0.74 GBq μmol^{-1} , American Radiolabeled Chemicals, St. Louis, MO) taken up in N₂ to yield ~ 5 MBq mL⁻¹. To avoid oxygen contamination, the mixture was stored over alkaline ascorbate (0.1 mol L⁻¹ sodium ascorbate in 0.1 mol L⁻¹ NaOH) as an oxygen scrubber. Before use in an experiment, portions of the mixture were transferred to Exetainers with N₂-degassed ultrapure water to avoid the risk of transferring alkaline ascorbate to the incubations. Here, the mixture was further amended with unlabeled methane to re-establish a methane pool during the incubations, as the original methane was stripped out during the degassing procedures described above. For the rate profiles, parallel incubations were performed with a lower and a higher addition of unlabeled methane aimed at final concentrations of 5 nmol L⁻¹ and 25 nmol L⁻¹, respectively. These concentrations were intended to bracket the predicted in situ concentration, based on published studies in the ETNP

(Pack et al. 2015; Chronopoulou et al. 2017) and our unpublished measurements from the region. However, analyses performed after the cruise revealed that the prepared ^3H methane tracer itself unexpectedly contained unlabeled methane corresponding to a final concentration of $\sim 75 \text{ nmol L}^{-1}$ and a specific activity of $16 \text{ MBq } \mu\text{mol}^{-1}$. Thus, incubations took place with methane concentrations of ~ 80 and 100 nmol L^{-1} , at the high end of those recorded at ETNP sites further south (Chronopoulou et al. 2017) and higher than in situ concentrations in the present study (see “Results” section). However, first-order kinetics has been demonstrated for aerobic methane oxidation in seawater at nanomolar concentrations (Ward et al. 1987; Reeburgh et al. 1991) and is generally assumed for calculation of in situ rates (e.g., Valentine et al. 2001; Steinle et al. 2015). We confirmed experimentally that first-order kinetics also applied in this study (see “Results” section). This allowed us to estimate in situ rates based on our measured rate constants and in situ methane concentrations (see “Scintillation counting and calculations” section). Results from the two methane additions were combined for these calculations. Experiments with oxygen sensitivity, time series, and inhibitors were conducted at $\sim 100 \text{ nmol L}^{-1}$ unlabeled methane and are presented as rate constants or accumulated radioactivity, independent of the methane concentration.

Methane kinetics experiments

The kinetics of methane oxidation were quantified in water from 130 and 300 m depth at Sta. 5 and 10. Two tracer/ N_2 mixtures were prepared with and without addition of unlabeled methane, respectively. A total of six different methane concentrations were obtained by further direct injection into the incubation vials of methane-saturated water and a 1:10 dilution of this in N_2 -degassed water. The volumes injected were determined based on the distribution coefficient (Wiesenburg and Guinasso 1979). The methane concentrations, covering a range of 69–525 nmol L^{-1} , were determined in a subset of the vials upon return to the home laboratory.

Oxygen sensitivity experiments

Experiments testing the oxygen sensitivity of methane oxidation were conducted at Sta. 8 and 10 with water from 130 and 300 m depth in the anoxic core. Oxygen was injected as air or oxygen-saturated water with injection volumes determined based on the temperature- and salinity-dependent distribution coefficient (Garcia and Gordon 1992). In addition to unamended control series, we included a set of vials incubated with addition of sodium dithionite as an oxygen scrubber (final concentration $\sim 7 \text{ } \mu\text{mol L}^{-1}$ from injection of a 0.6 g L^{-1} freshly prepared aqueous solution) to remove the remaining traces of oxygen. The aqueous oxygen concentration was measured during the incubation in a subset of vials mounted with trace range optode spots (TROXSP5, Pyroscience GmbH) using a Firesting fiber-optic oxygen meter (Pyroscience GmbH). The concentrations obtained with factory calibration were corrected for the zero reading obtained with addition of sodium dithionite at the end of the

experiment. In parallel to the oxygen and dithionite additions, these experiments further included a set of anoxic vials amended with $5 \text{ } \mu\text{mol L}^{-1}$ NH_4Cl to test for possible inhibitory effects of ammonium, which could arise if methane oxidation occurred via nonspecific activity of ammonium monooxygenases (Hyman and Wood 1983; Hyman et al. 1988).

Time course and inhibitor experiments

The time course of anaerobic methane oxidation was explored at Sta. 10 (130, 200, and 300 m) and Sta. T-North (40, 90, and 170 m) and the effect of two potential inhibitors was tested at two depths per station (130/200 m and 90/170 m, respectively) as part of the same experiment. N-allylthiourea (ATU) and 2-phenyl-4,4,5,5-tetramethylimidazole-1-oxyl 3-oxide (PTIO) were injected to final concentrations of $110 \text{ } \mu\text{mol L}^{-1}$ and $100 \text{ } \mu\text{mol L}^{-1}$, respectively. ATU inhibits bacterial ammonium monooxygenase and methane monooxygenase (Bédard and Knowles 1989; Martens-Habbena et al. 2015) while PTIO scavenges nitric oxide (NO) and thereby inhibits metabolisms in which NO is an intermediate, including archaeal ammonium oxidation (Martens-Habbena et al. 2015), anammox (Kartal et al. 2011), and, presumably, nitrite-dependent methane oxidation (Ettwig et al. 2010).

Scintillation counting and calculations

The activity of ^3H in water, $A_{\text{H}_2\text{O}}$, was determined by liquid scintillation counting of 4 mL aliquots after stripping off ^3H methane (Valentine et al. 2001). The stripping took place within 2 d of the termination of each experiment to minimize interference from the decomposition of the tracer (Bussmann et al. 2015). The activity of ^3H methane added was quantified in a subset of vials from each experiment from which methane had not been stripped. For this, 6 mL Exetainers served as scintillation vials. These were filled with scintillation fluid (UltimaGold™, Perkin Elmer) and subsequently amended with a $100 \text{ } \mu\text{L}$ air headspace by injection through the septum. A $20 \text{ } \mu\text{L}$ sample of headspace from the incubation vials was injected into the scintillation vials and allowed to equilibrate for 0.5 h on a rocking table before counting. Experiments showed that 90% of the gas was dissolved in the liquid, and counts were corrected for this fraction as well as for a shading effect (7%) from the cap of the vials. The activity of methane dissolved in the water during incubations, A_{CH_4} , was calculated from the headspace counts using the distribution coefficient (Wiesenburg and Guinasso 1979) and accounting for the different temperatures of incubation and analysis (14°C and 24°C , respectively) as well as the compression of the headspace resulting from injection of ZnCl_2 .

Methane oxidation rates were calculated following Reeburgh et al. (1991) and Valentine et al. (2001) as $k \times [\text{CH}_4]_{\text{in situ}}$ where k is the fractional turnover per unit time, which is equivalent to the rate constant when first-order kinetics apply. Thus, $k = (A_{\text{H}_2\text{O}} - A_{\text{H}_2\text{O control}}) \times (A_{\text{H}_2\text{O}} + A_{\text{CH}_4})^{-1} \times t^{-1}$, where t is incubation time and $A_{\text{H}_2\text{O control}}$ is the activity of the killed control after stripping of methane. Values of $A_{\text{H}_2\text{O control}}$ were $< 10 \text{ dpm mL}^{-1}$. As k varies between samples due to variation in the composition

and size of the methanotrophic community, we use the term apparent rate constant. For time course experiments, rates were calculated from the slope of linear regression lines of A_{H_2O} vs. time. A *t*-test was applied to determine if rates were significantly different from zero.

Sampling and extraction of DNA and RNA

Analysis of microbial DNA (16S rRNA gene amplicons) and RNA (metatranscriptomes) was used to identify microorganisms potentially contributing to methane oxidation in the ETNP OMZ. DNA analysis characterized community taxonomic composition along a depth gradient at Sta. 10 and T-North, while metatranscriptome analysis targeted two depths from the anoxic zone of these two stations (200 m from Sta. 10; 150 m from Sta. T-North), where we recorded some of the highest methane oxidation rates (see “Results” section).

Microbial biomass for DNA/RNA analysis was obtained following standard protocols in our lab (e.g., Padilla et al. 2016). Seawater from discrete depths (Table 2) spanning the oxycline and anoxic core was collected in Niskin bottles and returned to ship within 20 min of Niskin closing. Subsamples of Niskin water (5 L) were transferred to 20-liter Cubitainer® cartons, brought to an air-conditioned room, and filtered by peristaltic pump through 0.22 μ m pore-size Sterivex™ filters. After filtration (approximately 20 min), filters were filled with 1.8 mL RNA/DNA stabilizing buffer (25 mmol L⁻¹ sodium citrate, 10 mmol L⁻¹ EDTA, 5.3 mol L⁻¹ ammonium sulfate, pH 5.2), capped, flash-frozen in liquid nitrogen, and stored at -80°C.

DNA and RNA were extracted from replicate (subsamples from the same Niskin bottle) Sterivex™ filters as described previously (Padilla et al. 2016, 2017). For DNA extractions, cells were lysed by adding lysozyme (2 mg in 40 μ L of lysis buffer per filter) directly to the Sterivex™ cartridge, sealing the cartridge, and incubating for 45 min at 37°C. Proteinase K (1 mg in 100 μ L lysis buffer, with 100 μ L 20% sodium dodecyl sulfate) was added, and cartridges were resealed and incubated for 2 h at 55°C. The lysate was removed, and the DNA was extracted once with phenol:chloroform:isoamyl alcohol (25:24:1) and once with chloroform:isoamyl alcohol (24:1) and then concentrated by spin dialysis using Ultra-4 (100 kDa, Amicon) centrifugal filters.

The mirVana™ miRNA Isolation kit (Ambion) was used to extract RNA from the two filters for metatranscriptomics. Filters were thawed on ice, buffer was expelled and discarded, and cells were lysed by adding Lysis buffer and miRNA Homogenate Additive (Ambion) to the cartridges. The filters were vortexed and incubated on ice. Lysates were then transferred to RNAase-free tubes and RNA was separated via acid-phenol : chloroform extraction according to the kit protocol. Residual DNA was removed using the TURBO DNA-free™ kit (Ambion), and the extract was purified using the RNeasy MinElute Cleanup Kit (Qiagen).

16S rRNA gene sequencing and analysis

Sequencing of a variable fragment (V4) of the 16S rRNA gene was used to assess taxonomic composition. Amplicons

were synthesized by polymerase chain reaction (PCR) using equal amounts of DNA per reaction, Platinum® PCR SuperMix (Life Technologies), primers F515, and R806 recently modified from those of Caporaso et al. (2011) to limit biases against certain microbial groups and both appended with barcodes and Illumina-specific adapters according to Kozich et al. (2013), and the following thermal cycling protocol: denaturation at 94°C (3 min), followed by 30 cycles of denaturation at 94°C (45 s), primer annealing at 55°C (45 s) and primer extension at 72°C (90 s), followed by extension at 72°C for 10 min. Successful amplification was confirmed by gel electrophoresis, and amplicons purified using Diffinity RapidTip2 tips (Diffinity Genomics, NY). Amplicons from different samples were pooled at equimolar concentrations and sequenced on an Illumina MiSeq using a 500-cycle (2 × 250 bp) kit.

Paired end amplicon data sets were analyzed to detect amplicon sequence variants (ASVs) using DADA2 with default settings (Callahan et al. 2016). Briefly, filtering and trimming were performed with the DADA2 function “filterAndTrim” with the forward and reverse truncate lengths set to 240 and 160 for forward and reverse reads, respectively. The sequence count per sample was on average 27,863, with a high of 43,773 and a low of 3975 (Table 2). The resulting ASVs were checked for chimeras, and nonchimeric sequences (1679 ASVs across all data sets) were compared to the SILVA rRNA gene database (version 132) using nucleotide BLAST+ (version 2.3). To quantify ASV frequencies, all sample reads were then mapped to the 1679 ASVs using USEARCH with default sequences. The resulting “uc” table was used to construct a sample-ASV table using the script uc2otu.py. ASVs representing putative methanotrophic

Table 2. Summary of water sampling for, and number of reads per sample from, DNA and RNA analyses.

Station	Depth (m)	Volume (mL)	Read count
<i>16S rRNA gene amplicons</i>			
10	40	800	32,540
	60	800	24,404
	95	700	21,237
	110	1300	19,809
	130	1300	31,204
	200	650	3975
	300	700	31,891
	400	700	19,649
T-North	40	1500	38,222
	50	1500	43,773
	60	1600	34,654
	80	2000	30,428
	120	2100	19,809
	160	1600	38,487
<i>Transcriptomic non-rRNA</i>			
10	200	2000	4,835,694
T-North	150	700	8,737,815

taxa were identified by inspecting ASV taxonomic annotations (recovered from BLASTN analyses) using (1) keyword searches for known methanotrophic taxa and (2) manual parsing of all other ASVs to potentially identify taxa that have been implicated in methane cycling but are not canonical methanotrophic groups. Nonrarefied relative abundances of ASVs are reported per sample as a percentage of total reads mapping to the ASVs.

Metatranscriptome sequencing and analysis

Metatranscriptome data sets were generated by depleting rRNA from total RNA aliquots using the Ribo-Zero™ rRNA Removal Kit for bacteria (Epicenter), synthesizing cDNA using the ScriptSeq™ v2 RNA-Seq Library preparation kit (Epicenter), and MiSeq sequencing using a 500-cycle (2 × 250 bp) kit. Metatranscriptome data sets were mined to assess the potential activity of methanotrophic taxa and genes associated with methanotrophy. For the latter case, we focused on methane monooxygenase and methyl-coenzyme-M reductase-encoding genes (*pmo/mmo* and *mcr*) as markers of methanotrophy, as well as known genes of dissimilatory nitrogen metabolisms (see below). Prior to this analysis, metatranscriptome sequences were trimmed and merged as previously described (Padilla et al. 2017). Ribosomal RNA genes were identified and removed using riboPicker with default settings (Schmieder et al. 2012). Non-rRNA gene data sets of 4,835,694 and 8,737,815 reads for Sta. 10 (200 m) and Sta. T-North (100 m), respectively, were then used to analyze transcript function and proportional abundance. DIAMOND-BLASTX was used to query transcripts against a modified NCBI-RefSeq-Microbes database (updated January 2018), with the following search criteria: maximum number of target sequences = 1, bit-score > 40. RefSeq is a nonredundant database of genomes, transcripts, and proteins derived from a combination of culture-dependent and culture-independent studies (Pruitt et al. 2007). The most recent RefSeq version contains > 130 million nonredundant sequences, including from single-cell amplified genomes (SAGs) and metagenome-assembled genomes (MAGs) of OMZ microorganisms. For these searches, the RefSeq database was modified to include genomes of Methylococcaceae bacteria affiliated with methanotrophy in eastern Pacific OMZs (Tavormina et al. 2013; Padilla et al. 2017). Two Methylococcaceae genomes were included in our database (OPU3-MAG, genbank ID MPSY00000000.1, and B42-MAG-SAG co-assembly, genbank ID LSNW01000000), both of which were derived from marine environments. Contigs from these genomes were analyzed using the PROKKA automated bacterial genome annotation pipeline to identify protein-coding genes, which were then added to NCBI-RefSeq-Microbes. The final protein coding gene database contained 91,537,197 genes. DIAMOND-BLASTX results were outputted in tab format (format 6) to include NCBI annotations and taxonomic names, and then placed in a master table. Using keyword searches with “egrep,” the master table was queried to identify known methane-oxidizing taxa using the following search terms: egrep'(Methylomirab|NC10|Methylospira|Methylobacter|

Methyloldalium|Methylococcus|Methylococumis|Methylogaea|Methyloglobus|Methylomagnum|Methylomarinum|Methylomicrobium|Methylomonas|Methyloparacoccus|Methyl-oprofundus|Methylosarcina|Methylosarcina|Methylosoma|Methyl-oterricola|Methylovulum|Methylococcaceae|Methylothermaceae|Methylhalobius|Methylomarinovum|Methylothermaceae|Methyloumidiphilus|Methylococcales|OPU3|B42|Methanoper|methane|Methane|ANME)'. These results were then queried to identify genes of nitrate, nitrite, and nitric oxide cycling using egrep for the terms “nitrate,” “nitrite,” and “nitric.” A separate “egrep” search for methane monooxygenases was performed on the original master table to identify methane monooxygenases originating from organisms that may be of nonmethanotrophic origin (e.g., “uncultured archaea” are commonly used as taxonomic identifiers for clone based surveys). The results of the “methano-NOx” and “monooxygenase” searches were combined and used to generate our results. Transcripts matching each taxon were normalized by millions of reads per kilobase genome length per million reads mapped (RPKM), and transcript abundance per taxon was then plotted in R. All sequence data generated for this study can be accessed under BioProject ID PRJNA263621.

Results

Water column chemistry

At the off-shelf stations, anoxia prevailed from ~ 100 to 700–800 m depth (specific density, σ_θ , 26.0–27.15 kg m⁻³) and coincided with elevated nitrite concentrations, which reached a maximum of ~ 3 $\mu\text{mol L}^{-1}$ at ~ 130 m (26.2–26.3 kg m⁻³), while at the coastal site T-North, anoxia was reached already at 40 m depth (25.6 kg m⁻³) and the nitrite concentration increased from there towards the bottom at 180 m (Fig. 2a,c). The anoxic, nitrite-rich waters were further characterized by high methane concentrations that reached ~ 20 nmol L⁻¹ at the off-shelf sites and ~ 30 nmol L⁻¹ at T-North (Fig. 2b). A methane maximum was typically reached at 200–400 m depth (26.4–26.7 kg m⁻³) at the off-shelf stations, but two out of the three deep casts to > 500 m depth exhibited a second maximum at 600 m (27.05 kg m⁻³), with the concentration decreasing steeply to < 2 nmol L⁻¹ at the lower oxic-anoxic interface at 700–800 m. Methane concentrations above the anoxic core were higher than below, decreasing from 6–10 nmol L⁻¹ at the upper oxic-anoxic interface to 2–4 nmol L⁻¹ at the surface. Some casts showed maxima of 7–13 nmol L⁻¹ within the oxycline. These maxima were located at the depth of the primary nitrite maximum, where methane and nitrite concentrations correlated (Fig. 2b,c). Ammonium concentration was ≤ 100 nmol L⁻¹ at anoxic depths at all sites except T-North, where it reached 192 nmol L⁻¹ in the bottom water (data not shown).

Time course and kinetics of methane oxidation

Methane oxidation was detected in all incubations from anoxic depths. Tritium-labeled water from the oxidation of

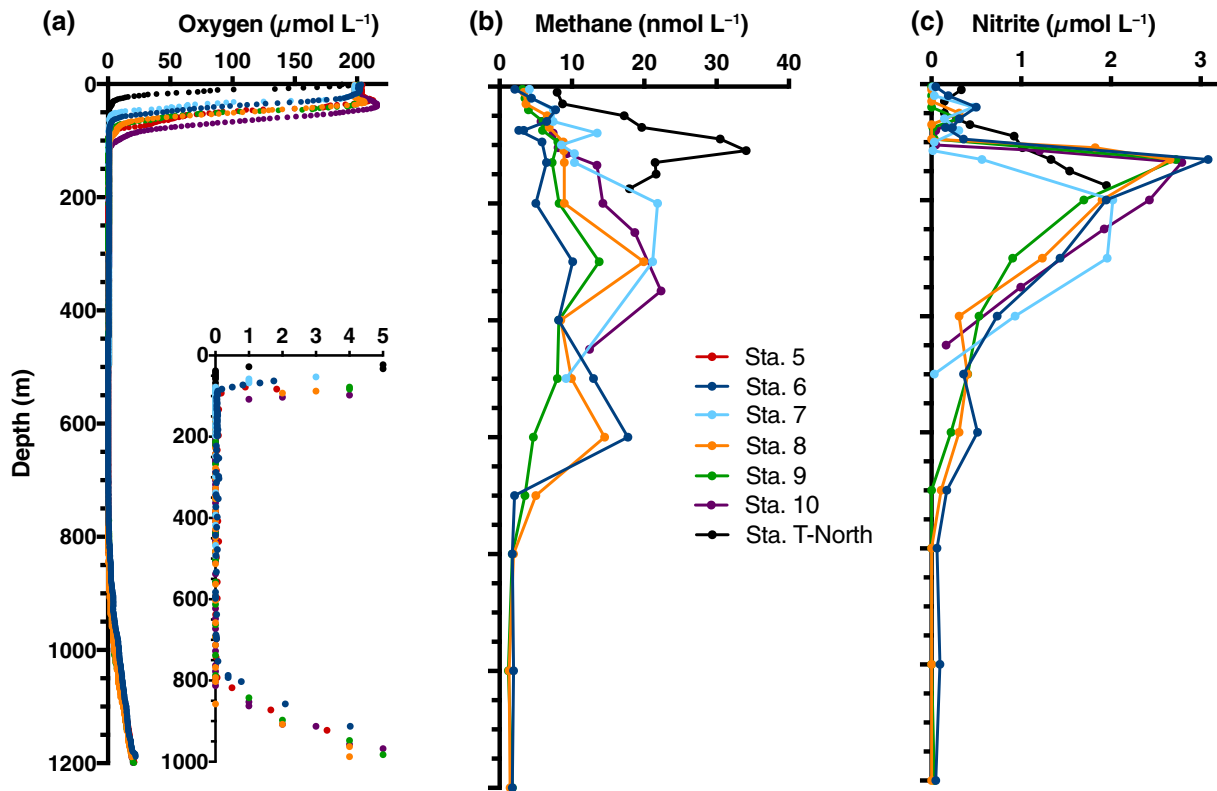


Fig. 2. Depth distributions of oxygen (a), methane (b), and nitrite (c) in the ETNP OMZ. Panel (a) shows oxygen profiles measured with a SBE43 sensor while the inset shows oxygen measured with a high-sensitivity STOX sensor. Methane data were not obtained for Sta. 5.

$^3\text{H-CH}_4$ accumulated linearly during the first 24–72 h during time course experiments, while activity accelerated markedly toward the end of the incubations, with acceleration at the coastal Sta. T-North occurring earlier than offshore at Sta. 10 (Fig. 3a,b). A similar acceleration during batch incubation has been observed for other microbial processes in OMZs and is generally considered as a “bottle effect” with the initial rates assumed to reflect in situ activity more accurately than rates during the acceleration period (e.g., Thamdrup et al. 2006;

Garcia-Robledo et al. 2016). Accordingly, all rates and rate constants reported here are based on 24 h incubations.

Methane oxidation rates increased approximately linearly with increasing added methane concentrations up to $0.5 \mu\text{mol L}^{-1}$ without any indication of saturation (Fig. 4). This confirmed the general assumption of first-order kinetics (Reeburgh et al. 1991; Valentine et al. 2001) and justified our calculation of methane oxidation rates based on the apparent rate constant k determined for each sample and the in situ concentration.

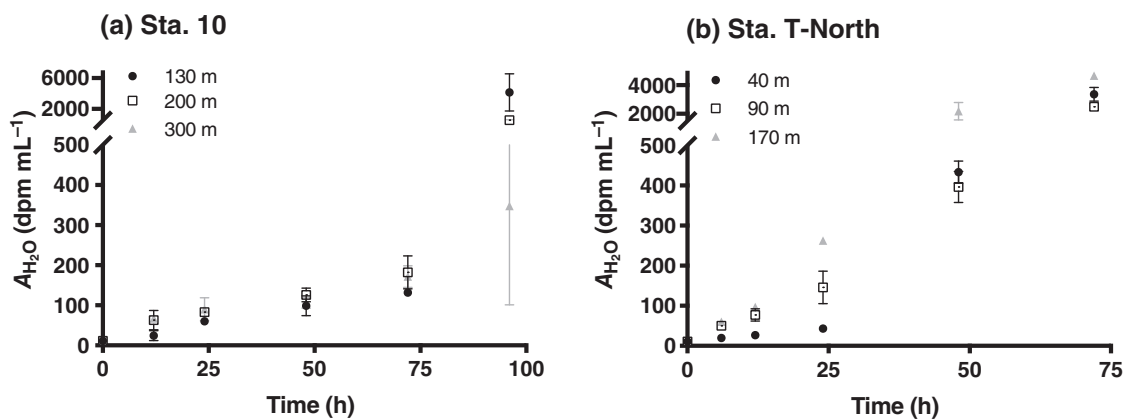


Fig. 3. Time courses of methane oxidation in incubations of water from different anoxic depths at Sta. 10 (a) and Sta. T-North (b). The y-axis represents the accumulation of ^3H -labeled water. Error bars represent standard errors ($n = 3$).

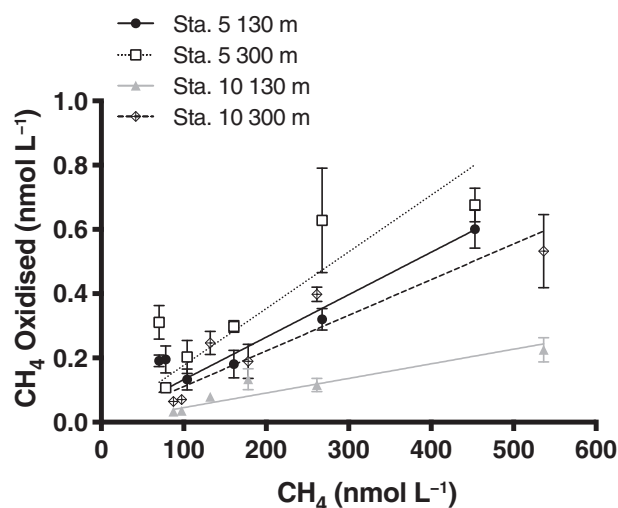


Fig. 4. Validation of first-order kinetics of methane oxidation in incubations with different amounts of methane added. Regression lines for each of the four experiments are shown. Error bars represent standard error.

Depth distribution of methane oxidation

The apparent rate constant of methane oxidation increased abruptly below the oxic-anoxic interface with the increase largely paralleling the increase in nitrite concentration (Fig. 5b). While the apparent rate constant was $< 0.15 \text{ yr}^{-1}$ above the interface, it reached a broad maximum of $\sim 1 \text{ yr}^{-1}$ between the secondary nitrite maximum at 130 m and the center of the OMZ core at 300 m at both of the off-shelf stations, while the highest value of 2.4 yr^{-1} was determined in the bottom water at T-North (Fig. 5b). As the methane concentration did not change dramatically across the oxic-anoxic interface, the methane oxidation rate showed a similar depth distribution as the apparent rate constant with a maximum of $0.04\text{--}0.05 \text{ nmol L}^{-1} \text{ d}^{-1}$ at 250 m depth at both Sta. 8 and 10 and the highest rate of $0.12 \text{ nmol L}^{-1} \text{ d}^{-1}$ at Sta. T-North (Fig. 5a,c).

Sensitivity to oxygen and inhibitors

The anaerobic nature of the measured methane oxidation activity in the OMZ core waters was further emphasized by oxygen addition experiments, which consistently showed an inhibitory effect already at $0.5 \mu\text{mol L}^{-1}$ oxygen (Fig. 6a). The inhibition was most pronounced at Sta. 8 reaching $\geq 90\%$ already at $1\text{--}2 \mu\text{mol L}^{-1} \text{ O}_2$, whereas $\sim 20\%$ of the activity remained at $10 \mu\text{mol L}^{-1} \text{ O}_2$ at Sta. 10. Addition of dithionite as an oxygen scavenger stimulated methane oxidation relative to the control treatment in three of four experiments while in one case the rate with dithionite did not differ from the control (Fig. 6b).

Apart from oxygen, PTIO was the only substance with an inhibitory effect on methane oxidation, with $100 \mu\text{mol L}^{-1}$ amendments inhibiting the process by 61–62% in three experiments and by 86% in the fourth one (Fig. 7). By contrast, the addition of $5 \mu\text{mol L}^{-1}$ ammonium as a potential competitive

inhibitor of methane oxidation had no discernable effect in any of the four experiments (Fig. 6b), and $110 \mu\text{mol L}^{-1}$ ATU also did not inhibit methane oxidation (Fig. 7). Instead, ATU stimulated the process significantly in one case, and there was a trend toward stimulation in two of the three other experiments.

DNA and RNA analyses

Analysis of 16S rRNA gene amplicons detected three methanotroph-related ASVs from Sta. 10 and T-North (Fig. 5d–f). These included sequences most closely related to NC10 (ASV 1190) and to the environmental clades OPU1 and OPU3 (Tavormina et al. 2013) of the Methylococcales bacteria (ASV 1471 and 1150, respectively). All three of these ASVs occurred at relatively low proportional abundance but reached maximal proportional representation (0.03–0.06%) at 400 m depth in the anoxic core at Sta. 10. However, the Methylococcales ASVs also exhibited local abundance peaks at ~ 100 m depth in the oxycline and upper OMZ above the secondary nitrite maximum, whereas the NC10 ASV was not detected at those depths.

Methanotroph sequences were also recovered in anoxic zone metatranscriptomes from both Sta. 10 and T-North (Fig. 8). In both data sets, the most abundant genes in the methanotroph-affiliated transcript pool were associated with dissimilatory nitrogen metabolism, including genes that, based on our analytical approach, are most closely related to those encoding the nitric oxide reductase of NC10 and the respiratory nitrate reductase of Methylococcales bacteria and ANME-2d archaea related to “*Candidatus* Methanoperedens sp.” Genes of methane oxidation, notably encoding PMO, were also detected, albeit at lower abundance. Several of the detected PMO variants were most closely related to those from Methylococcales bacteria (e.g., *Methylobacter*, *Methylocaldum*, *Methylococcus*, *Methylosarcina* sp. in Fig. 8), whereas neither NC10-related PMO genes nor ANME-2d-related methyl coenzyme-M reductase genes were detected. The most abundant PMO transcripts detected were identified as belonging to *Nocardioides* and *Streptomyces* of the Actinobacteria, which are not known as methanotrophs.

We caution that the taxonomic affiliations of the proteins identified in our transcript analysis reflect those of the most similar homologs in the reference databases used in this study. Thus, the annotations are based on matches to the curated RefSeq database, followed by validation with targeted searches against the NCBI-nr database. While genomes of OMZ microbes are included in the RefSeq database, this representation is far from complete (as is the case for many natural environments) and does not yet include, for example, a marine NC10 representative. It is inevitable that knowledge of the taxa and functional genes associated with OMZ methane oxidation will improve as additional curated genomes are made available. Doing so, however, will remain a challenge for taxa

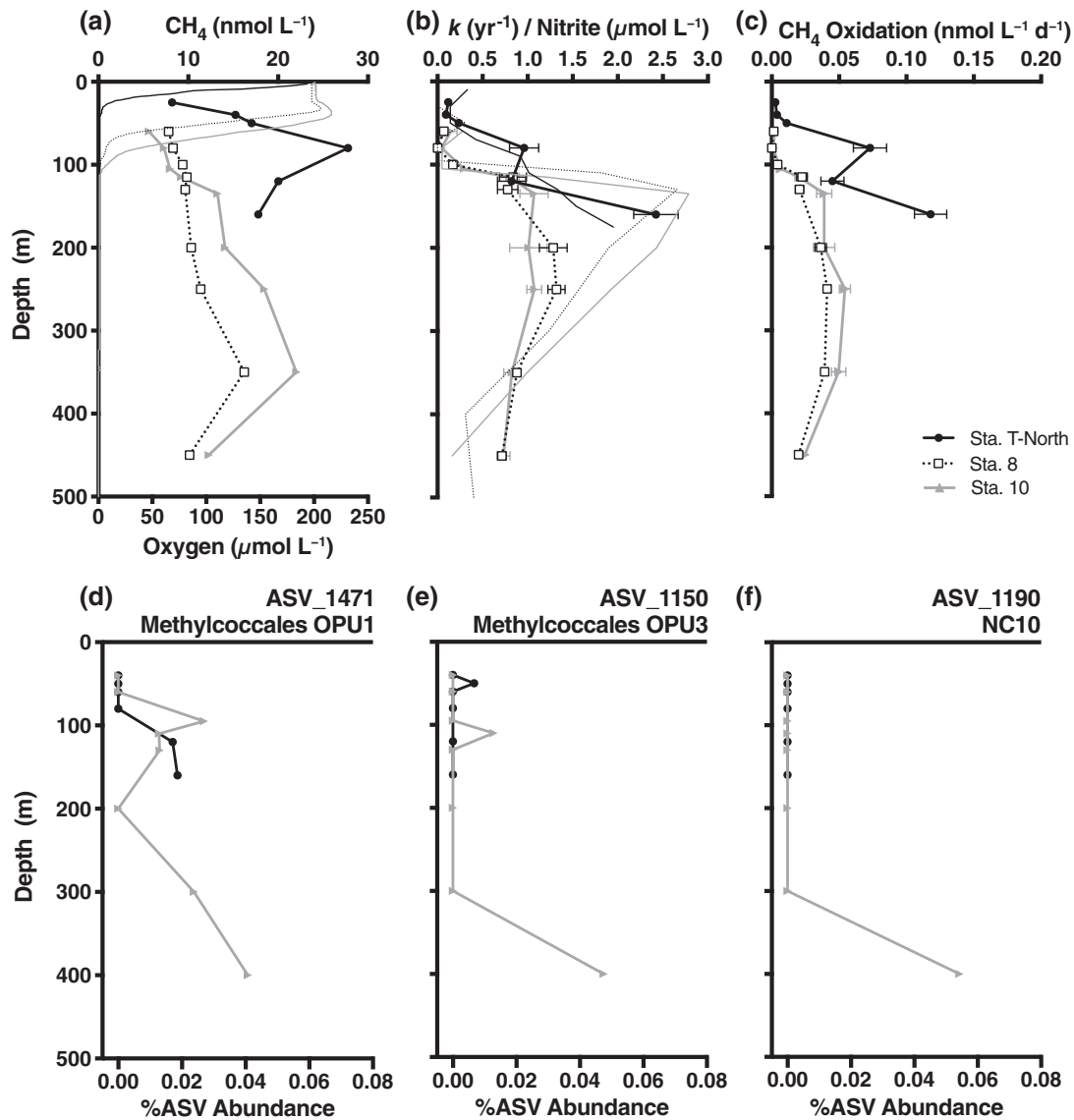


Fig. 5. Top panels: Vertical profiles of oxygen (curves without symbols) and methane (with symbols) concentrations (a), nitrite concentrations (without symbols) and apparent rate constants of methane (with symbols) (b), and rates of methane oxidation (c) at the shelf site T-North and off-shelf Sta. 8 and 10. Error bars represent standard error. Bottom panels: Depth distributions of the relative abundance of three ASVs of methanotrophs identified through 16S rRNA gene amplicon sequencing at Sta. T-North and Sta. 10. (d) ASV 1471 related to Methylococcales clade OPU1; (e) ASV 1150 related to Methylococcales clade OPU3; (f) ASV 1190 related to NC10 bacteria.

such as NC10 that are present at low frequency and therefore unlikely to be recovered in genomic or metagenomic surveys.

Discussion

Our results provide experimental evidence for a substantial anaerobic methane sink in the OMZ of the ETNP and suggest a coupling to the nitrogen cycle potentially catalyzed by nitrite-reducing members of the NC10 clade, but also with potential roles for Methylococcales bacteria, and nitrate-reducing ANME-2d archaea. As discussed below, the measured apparent rate constants of anaerobic methane oxidation imply

that microbial consumption exceeds mixing as a sink for methane in the OMZ core.

Evidence for anaerobic methane oxidation

The steep increase in rates and apparent rate constants of methane oxidation across the oxic-anoxic interface and into the OMZ core links this activity to the anoxic, nitrite and methane rich environment of the core (Fig. 5). As the apparent rate constant is expected to scale with population size, the depth distribution of methane oxidation further indicates that the OMZ core is the niche for a distinct population of

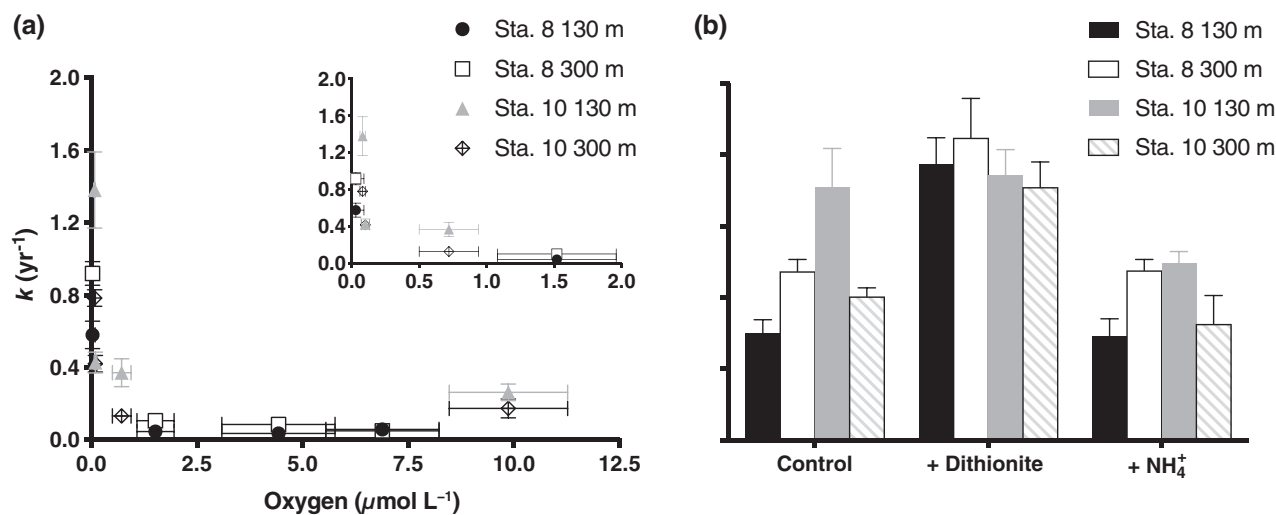


Fig. 6. (a) Oxygen sensitivity of the rate constant of methane oxidation from experiments with oxygen additions with an inset showing an expanded version of the low concentrations. Vertical error bars represent standard error. Horizontal error bars represent the standard deviation of oxygen concentrations measured during the incubation. (b) Comparison of rate constants of methane oxidation measured without amendment ("control"; corresponds to the lowest oxygen concentrations in a) and with the addition of dithionite or ammonium. Error bars represent standard error.

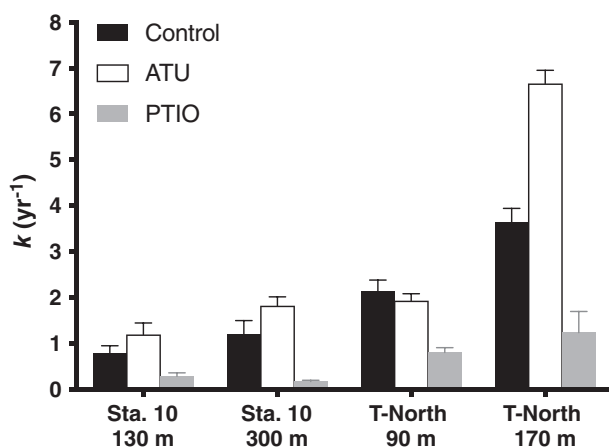


Fig. 7. The effect of potential inhibitors ATU (allylthiourea) and PTIO (2-phenyl-4,4,5,5-tetramethylimidazole-1-oxyl-3-oxide) on the rate constant of methane oxidation compared to unamended controls. Error bars represent standard error.

methane oxidizers, which therefore are presumably at lower abundance in oxic waters. The persistence of anoxia from ~ 100 to 700–800 m depth in the northern part of the ETNP OMZ is well documented (Fig. 2a, Tiano et al. 2014, Ganesh et al. 2015, Padilla et al. 2016). Oxygen at nanomolar levels is occasionally observed in layers below ~ 500 m depth at offshore sites as well as in the secondary chlorophyll maximum, which is typically intermediate between the oxic-anoxic interface and the secondary nitrite maximum (Tiano et al. 2014; Garcia-Robledo et al. 2017). However, the highest rates and apparent rate constants for methane oxidation were found between the maxima in nitrite and methane (Fig. 5) in the center of the anoxic core at the off-shelf stations, rather than at the fringes where

transient presence of oxygen due to either mixing or photosynthesis is more likely. This suggests an anaerobic metabolism for the methane oxidizers in the OMZ core.

The anaerobic nature of methane oxidation was further indicated by the inhibitory effect of low amounts of added oxygen in incubations from the anoxic OMZ core (Fig. 6a). Despite severe precautions, contamination with low nanomolar amounts of oxygen appears inevitable in shipboard incubations of OMZ waters (Ganesh et al. 2015) and could potentially support microaerophilic methane oxidation as observed experimentally in lakes and coastal waters (Blees et al. 2014; Oswald et al. 2015; Steinle et al. 2017). The inhibition of methane oxidation by oxygen was stronger, however, than previously reported from coastal hypoxic waters (Steinle et al. 2017), and the neutral to stimulatory effect of oxygen-scavenging dithionite further argues for an anaerobic rather than a microaerobic pathway (Fig. 6b). The stimulation observed in three of four dithionite experiments is likely attributed to the removal of low but still partially inhibitory levels of oxygen present in the incubations (≤ 75 nmol L⁻¹). Alternative effects of dithionite or sulfur compounds formed by dithionite oxidation cannot be excluded, though mechanisms for such effects are not obvious. Oxygen addition experiments were only carried out with samples from the anoxic core. In the oxycline and at the oxic-anoxic interface, where a peak in the abundance of Methylococcales was observed (Fig. 5d, e), a positive response to oxygen might be expected. Indeed, the very low rates of methane oxidation obtained in our anoxic incubations from these depths (≤ 0.004 nmol L⁻¹ d⁻¹; Fig. 5c) could be the result of oxygen limitation.

The steep increase in rates below the oxic-anoxic interface (Fig. 5) contrasts with the observations in a previous study in the southern half of the ETNP OMZ (Fig. 1), which found a

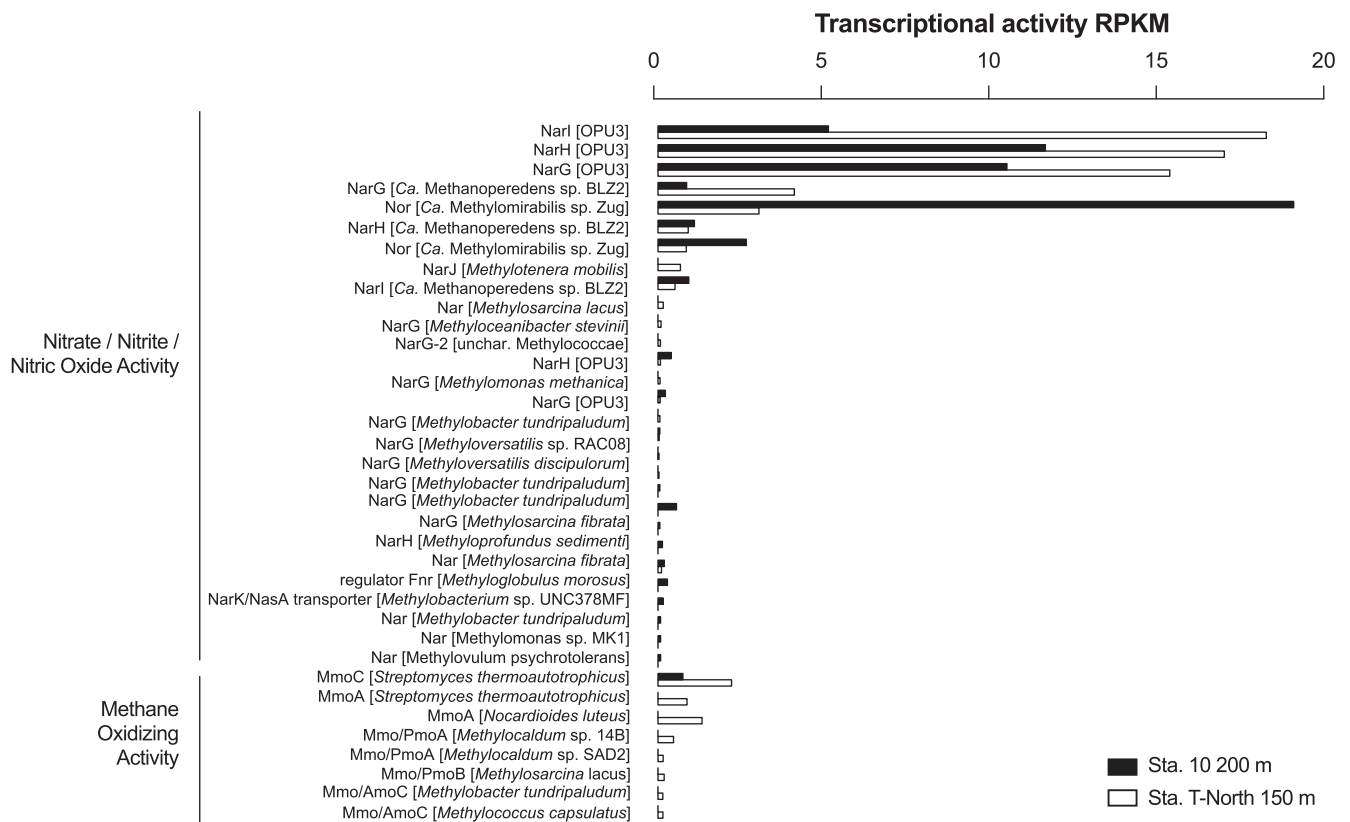


Fig. 8. Results of transcriptome analyses. Normalized abundance of transcripts encoding components of enzymes involved in dissimilatory nitrate, nitrite, and nitric oxide transformations in methanotrophic taxa, and in methane oxidation (see text for details). Transcriptomes were obtained from anoxic depths at the shelf Sta. T-North and off-shelf Sta. 10. Transcript abundance is given as millions of RPKM.

positive correlation between methane oxidation rates and oxygen, and suggested that the process is subject to second-order kinetic control from the combined availability of methane and oxygen (Pack et al. 2015). In that study, the in situ oxygen concentration for most samples was $\geq 2 \mu\text{mol L}^{-1}$, but the anoxic core may have been transected at two or three of the eight sites, based on the observed typical “flatlining” of oxygen profiles (cf. Thamdrup et al. 2012) and accumulation of methane. As special precautions were not taken in that study to avoid oxygen contamination during sampling, and as sampling in and subsampling from Niskin bottles typically results in contamination on the order of $1 \mu\text{mol L}^{-1}$ oxygen (E. Garcia-Robledo and B. Thamdrup unpubl. results), it is likely that any anaerobic methane oxidizing activity was inhibited during the incubations.

Pathways and organisms involved in anaerobic methane oxidation

Nitrate and nitrite are the most favorable terminal electron acceptors for microbial respiration in the anoxic OMZ core and are thereby likely oxidants for methane there. The inhibitory effect of the nitric oxide scavenger PTIO (Fig. 7) suggests that methane oxidation is at least partially coupled to a metabolism involving nitric oxide. The only anaerobic methane oxidizers known to utilize nitric oxide are species of “*Cand.*

Methyloirabilis” of the NC10 clade, which are thought to produce nitric oxide through nitrite reduction and consume it by dismutation into N_2 and O_2 , the O_2 subsequently being used for the oxidation of methane to methanol (Ettwig et al. 2010). Given the critical role of nitric oxide, we expect an inhibitory effect of PTIO on methane oxidation by NC10 bacteria, and our observations thus hint at their involvement. Yet we cannot with certainty link the observed effect to this clade, as a direct demonstration of the effect of PTIO on NC10 bacteria is still pending. Other, unknown organisms that couple methane oxidation to NO dismutation or even to the classical denitrification pathway, including NO reduction, could also be involved. Also, while a PTIO concentration of $100 \mu\text{mol L}^{-1}$ was chosen based on its ability to inhibit ammonium oxidation in Archaea, in which nitric oxide is also a critical intermediate (Martens-Habben et al. 2015), the incomplete inhibition observed here cannot be taken as evidence for the activity of other pathways before a dose-response relationship for NC10 bacteria has been established.

Methane oxidation could potentially also be affected by PTIO if coupled to denitrification as described, e.g., for aerobic *Methylomonas denitrificans* of the Methylococcales under extreme hypoxia (Kits et al. 2015). This organism reduces nitrate to nitrous oxide by the canonical denitrification pathway, but it is still assumed to require oxygen for the initial

activation of methane. Such organisms are therefore not expected to thrive on methane in the anoxic OMZ core, although our molecular results suggest that they may also be present and transcriptionally active at anoxic depths (see below). In addition, as energy conservation is coupled to the reduction of both nitrate and nitrite during denitrification, the scavenging of nitric oxide would not necessarily inhibit methane oxidation. Indeed, nitric oxide appeared to be the end product of nitrate reduction in Methylococcales methanotrophs identified through metagenomics near the oxic-anoxic interface of an OMZ-like coastal basin (Padilla et al. 2017). A metabolism of this type is therefore less likely to explain the observed effect of PTIO.

The involvement of NC10 bacteria in anaerobic methane oxidation in the ETNP OMZ was previously indicated by their presence and transcriptional activity in the anoxic core (Padilla et al. 2016). The similarity in the depth distribution of methane oxidation activity at Sta. 8 and 10 (Fig. 5b, c), and the abundance of NC10 bacteria determined at the same locations in 2014 based on copy numbers of the 16S rRNA gene (Padilla et al. 2016), provides further support for a role of NC10 bacteria in the process. Similar to the rate constant, copy numbers increased steeply below the upper oxic-anoxic interface and reached maxima between 200 and 400 m depth before decreasing toward the lower boundary of the OMZ core. Gene copy numbers of up to $\sim 100 \text{ mL}^{-1}$ and a reported specific methane oxidation rate of $0.09\text{--}0.2 \text{ fmol CH}_4 (16\text{S rRNA gene})^{-1} \text{ d}^{-1}$ for NC10 bacteria (Ettwig et al. 2009), corresponds to methane oxidation rates in the range of $0.009\text{--}0.02 \text{ nmol L}^{-1} \text{ d}^{-1}$. This range is in reasonable agreement with the rates measured here ($0.03\text{--}0.06 \text{ nmol L}^{-1} \text{ d}^{-1}$ at 130–350 m), considering that quantification of genes from natural environments is likely to be affected by factors such as extraction efficiency and primer coverage and that just a single determination of specific metabolic rates of NC10 bacteria is available from a freshwater culture, while such rates may vary between strains from different environments. Shotgun metagenomic sequencing has failed to recover NC10 from the ETNP OMZ (Fuchsman et al. 2017), consistent with our prior quantitative PCR-based cell counts indicating this group accounts for $\leq 0.01\%$ of the total bacterial population (Padilla et al. 2016). While NC10 are clearly part of the rare biosphere in this system, the above calculations nonetheless suggest that this group could be the main contributor to anaerobic methane oxidation in the ETNP OMZ.

To further explore this hypothesis, taxonomic and transcriptomic analyses were employed to test for evidence for a role for NC10, as well as potential contributions from other methane oxidizing taxa. Sequencing of the community 16S rRNA gene pool revealed three methanotroph-related ASVs that peaked in abundance at anoxic depths (Fig. 5d–f). These included variants related to NC10, as well as gammaproteobacteria of the Methylococcales related to clades OPU1 and OPU3. All of these ASVs occurred at low abundance (typically less than 0.06%) with maxima at 400 m at Sta. 10 and, for the two Methylococcales variants, near the oxic-anoxic interface. For the NC10 bacteria, their

detection in the OMZ core agrees with the prior results suggesting a distribution linked to the anoxic, methane- and nitrite-enriched zone (Padilla et al. 2016). Furthermore, their low relative abundance indicated by quantitative PCR ($\leq 0.01\%$; Padilla et al. 2016) may explain the lack of NC10-related amplicons at most depths considering total amplicon sequence counts of $0.4\text{--}4 \times 10^4$ per sample (Table 2). For the Methylococcales ASVs, the peaks in relative abundance near the oxic-anoxic interface at ~ 100 m depth at Sta. 10 and, for ASV 1150 (OPU3), at 50 m at T-North are consistent with a previous observation of peaks in abundance of the OPU1 and OPU3 clades at the upper and lower boundary of the low-oxygen core in the southernmost part of the ETNP OMZ (Tavormina et al. 2013), as well as with evidence that denitrifying Methylococcales in OMZs predominantly inhabit oxycline or upper OMZ depths where low oxygen may be available for methane oxidation (Padilla et al. 2017). The highest relative abundance of ASV 1471 (OPU1) at both stations and of ASV 1150 (OPU3) at Sta. 10 was, however, found at the depths furthest separated from the oxic-anoxic boundaries where aerobic metabolism cannot be sustained, though the depth of this peak did not match the peak in methane oxidation rates (Fig. 5c). A prior amplicon-based survey of these sites detected neither Methylococcales nor NC10-related sequences in the OMZ core (Padilla et al. 2016); however, a comparison between that study and the current results is challenging, as the prior work used a shallower sequence depth per sample ($\sim 1/4$ of the depth used here) and classified sequences using a different taxonomic database (Greengenes).

Evidence that NC10 bacteria and members of Methylococcales were not only present but also active in the anoxic OMZ was provided by the metatranscriptome analysis at Sta. 10 and T-North, where the most abundant transcripts associated with methanotrophy linked to denitrification steps were affiliated with nitrite-dependent NC10 metabolism and with nitrate reduction by members of the Methylococcales (Fig. 8). Notably, transcripts encoding variants of the NC10 nitric-oxide (NO) reductase-like enzyme, which is hypothesized to mediate NO dismutation into N_2 and O_2 (Ettwig et al. 2010; now often called NO dismutase), were abundant in the methanotroph-affiliated transcript pool. These variants fall within a broad clade of aberrant NO reductases commonly referred to as qNor-like reductases (Fuchsman et al. 2017). Here, the transcripts most closely matched qNor-like NO-reductases/putative dismutases of the NC10 representative “*Ca. Methyloimabilis limnetica*” from Lake Zug (Graf et al. 2018). However, multiple qNor-like variants with close phylogenetic relationships to the NO reductase/dismutase of NC10 have been recovered from the ETNP OMZ and recently shown to cluster into discrete subclades, suggesting a diversity of organisms may carry these genes, and potentially have acquired them by lateral transfer (Fuchsman et al. 2017). Additional long contig or whole genome data will be required to definitively link these diverse variants to methane oxidation potential.

Consistent with the results of Padilla et al. (2016), we did not recover transcripts encoding the PMO of NC10 bacteria (Fig. 8),

suggesting either minor transcriptional activity of NC10 methane oxidation genes, or potential unique PMO variants that escaped detection by queries against the currently available NC10 reference genes (from non-OMZ relatives). Rather, the recovered PMO transcripts, albeit at low frequencies compared to nitrate reduction genes, were associated with Gammaproteobacteria of the Methylococcales or, surprisingly, with Actinobacteria of the genera *Nocardiodides* or *Streptomyces*, with the latter being the most abundant PMO variant. However, when queried (BLASTX) against the entire NCBI-nr database (rather than RefSeq), these *Streptomyces*-annotated transcripts matched, with highest bit-scores and coverage values, to the candidate phylum “Rokubacteria” (Anantharaman et al. 2018), which was previously identified in metagenomes from diverse terrestrial habitats (Becraft et al. 2017). The group appears metabolically versatile, but like for Actinobacteria there is no direct evidence for methane oxidation in this group, and the annotation of these monooxygenases remains hypothetical. The taxonomic annotation of all other PMO transcripts did not change upon verification against NCBI-nr, confirming that at least some component of the OMZ PMO pool is linked to gammaproteobacteria. Nonetheless, without phylogenetically vetted whole genomic data from microbes at our study site, the taxonomic identities assigned here to functional gene transcripts should be interpreted as preliminary. A role for gammaproteobacterial methanotrophs was also supported by the detection of relatively high numbers of transcripts encoding dissimilatory nitrate reductases affiliated with the OPU3 cluster (family Methylococcaceae) of Methylococcales (Fig. 8). In prior work in the Golfo Dulce, denitrification-related transcripts from OPU3 peaked in relative abundance just below the oxic-anoxic interface (Padilla et al. 2017). Here, however, metatranscriptome samples were collected from deep within the anoxic core, at considerable vertical distance (> 100 m) from the oxycline. Together with the deep maxima in 16S rRNA gene amplicons (Fig. 5d,e), our observations suggest that these gammaproteobacterial methanotrophs may contribute to methanotrophy in the ETNP, but they also raise the question of how these organisms obtain oxygen for methane activation or otherwise sustain their metabolism. A similar conundrum relates to the abundance and activity of gammaproteobacterial methanotrophs in deep anoxic lake waters (Oswald et al. 2016).

Interestingly, we also recovered relatively high numbers of nitrate reductase-encoding transcripts affiliated with “*Candidatus* Methanoperedens nitroreducens,” a nitrate-reducing, anaerobic methane-oxidizing archaeon of the ANME-2d clade (Haroon et al. 2013; Berger et al. 2017; Fig. 8). To our knowledge, ANME-2d associated with “*Cand.* Methanoperedens” were not previously reported from OMZ waters. In methane and nitrate-fed bioreactors, ANME-2d and NC10 bacteria are co-enriched, with nitrate reduction by ANME-2d supporting nitrite-dependent methane oxidation by NC10 (Raghoebarsing et al. 2006; Haroon et al. 2013). Such a dependency is not likely in the OMZ, however, because nitrite is mainly supplied by organotrophic nitrate reduction, as discussed below. While it is tempting to speculate that

ANME-2d are present and could be performing nitrate reduction coupled to methane oxidation, nitrate reductases are known to undergo extensive horizontal gene transfer and are therefore not ideal markers of taxonomic affiliation. Nonetheless, these preliminary results are intriguing and merit follow-up investigations with more extensive sequence data.

Together, our molecular results, notably the taxonomically informative 16S rRNA gene data, support the previously indicated role of NC10 bacteria as potential contributors to methane oxidation in the ETNP OMZ (Padilla et al. 2016; Chronopoulou et al. 2017). The transcript data also raise the possibility that other anaerobes, such as ANME-2d, may contribute to this process, although this conclusion was not supported with either coupled 16S rRNA gene data or the detection of *mcr* genes, and therefore should be considered preliminary. By contrast, although the Methanococcales are present and transcriptionally active, it is not clear if or how they might contribute to methane oxidation in the anoxic OMZ core because of their presumed oxygen requirement for methane activation via PMO. Alternatively, these organisms might survive anaerobically on other substrates (e.g., Dam et al. 2013). Also the high sensitivity of the process to oxygen observed in our experiments (Fig. 6) implicates obligate anaerobes, potentially NC10, as the more likely conveyors of this process.

Anaerobic methane oxidation and the OMZ nitrogen and methane budgets

The maximal anaerobic methane oxidation rate at the off-shelf sites ($0.05 \text{ nmol L}^{-1} \text{ d}^{-1}$; Fig. 5) was 1–2 orders of magnitude lower than denitrification rates previously determined at similar locations in the northern ETNP OMZ ($0.5\text{--}4 \text{ nmol L}^{-1} \text{ N d}^{-1}$; Babbín et al. 2014; Ganesh et al. 2015). Thus, considering the 1:2.7 methane:nitrite ratio of anaerobic methane oxidation coupled to nitrite reduction by NC10 bacteria, these organisms cannot account for much more than 10% of the N_2 production through denitrification. As anammox and denitrification make similar contributions to N_2 production in the region (Babbín et al. 2014; Ganesh et al. 2015, 2018), the contribution of nitrite-dependent anaerobic methane oxidation to the total loss of reactive nitrogen would be about half of this value, and the fraction would be even smaller if methane oxidation is to some extent also coupled to nitrate reduction as hinted by the “*Ca.* Methanoperedens” transcripts. Thus, anaerobic methane oxidation appears to play a very minor role in the reactive nitrogen budget of the ETNP OMZ.

In contrast to its lack of importance for nitrogen cycling, anaerobic methane oxidation appears to contribute substantially to the methane budget in the OMZ. The rates of anaerobic methane oxidation measured here, $0.004\text{--}0.12 \text{ nmol L}^{-1} \text{ d}^{-1}$ at anoxic depths (Fig. 5), are near the geometric mean of the wide range of aerobic methane rates previously reported for marine waters (10^{-5} to $10^3 \text{ nmol L}^{-1} \text{ d}^{-1}$; Mau et al. 2013). Much of the variability within this wide range is related to variations in methane concentrations, with particularly high rates associated with methane plumes (e.g., Valentine et al. 2001; Steinle et al.

2015). A more detailed understanding of the efficiency of the process can be gained from comparison of apparent rate constants, in accordance with the first-order kinetics of the process (Fig. 4). The rate constants measured here ($0.2\text{--}2.4\text{ yr}^{-1}$ at anoxic depths, depth-weighted average 0.94 yr^{-1} and 0.87 yr^{-1} at Sta. 8 and 10, respectively; Fig. 5) were intermediate between those estimated for open ocean settings ($0.02\text{--}0.1\text{ yr}^{-1}$) and vent/seep-influenced or coastal environments ($1\text{--}30\text{ yr}^{-1}$; Valentine et al. 2001; Heintz et al. 2012; Steinle et al. 2015), and comparable to those determined for aerobic oxidation in, e.g., the Eel River Basin ($0.4\text{--}1.1\text{ yr}^{-1}$ at basin depths; Valentine et al. 2001) and at midwater depths in the California Borderland Basins (approximately $0.4\text{--}1.7\text{ yr}^{-1}$; Heintz et al. 2012). The average rate constants are also within the range of average values from surface waters in the southern part of the ETNP OMZ ($0.2\text{--}3.3\text{ yr}^{-1}$), with the lower and higher values of this range representing results from $^{14}\text{C}\text{-CH}_4$ and $^3\text{H}\text{-CH}_4$ based incubations, respectively (Pack et al. 2015). Thus, anaerobic methane oxidation in the ETNP OMZ did not appear much less efficient than its aerobic counterpart.

The relatively high apparent rate constants of anaerobic methane oxidation in the ETNP OMZ contradict previous suggestions that the accumulation of methane in the OMZ results from the advection from a coastal source with little or no consumption due to oxygen limitation (Sansone et al. 2001, 2004). Notably, the average rate constants at anoxic depths of Sta. 8 and 10 correspond to a turnover time with respect to oxidation ($\tau = k^{-1}$) of $1.1\text{--}1.2\text{ yr}$, which is substantially faster than the estimated replacement time of the ETNP OMZ water mass of $3.9 \pm 0.8\text{ yr}$ (DeVries et al. 2012). Assuming that the rate constants are representative of the entire ETNP OMZ core, this implies that methane loss by anaerobic oxidation dominates over loss by mixing as a sink for methane, with $\sim 80\%$ of the methane input to the OMZ core being consumed internally by microbes. This is a first approximation, which should be refined, e.g., by more detailed mapping of methane concentrations and rate constants. The rate constant of anaerobic methane oxidation is expected to correlate with the abundance of NC10 bacteria to decrease with increasing distance from shore has been observed (Padilla et al. 2016), a parallel gradient in k might be expected. In the previous study, however, Sta. 8 and 10, used for our extrapolation here, had substantially lower average abundances of NC10 16S rRNA gene copies at anoxic depths than a station closer to shore, and Sta. 10 had the lowest abundance of all stations examined. Thus, with the limited evidence available, an extrapolation based on these stations appears realistic at least for the northern part of the ETNP OMZ (Fig. 1). We thus conclude that the OMZ methane pool is dynamic and the flux to the surrounding oxic waters is strongly attenuated by the anaerobic sink.

Applying a rate constant of 0.9 yr^{-1} to the 0.3 Tg methane inventory of the ETNP OMZ (Sansone et al. 2001) yields an anaerobic methane sink of 0.27 Tg yr^{-1} . This is within the range of the

integrated methane oxidation rate of $0.05\text{--}1\text{ Tg yr}^{-1}$ for $200\text{--}760\text{ m}$ depth in the region estimated by Pack et al. (2015), which again emphasizes the efficiency of anaerobic oxidation. When the water residence time of the ETNP OMZ is further taken into account, we arrive at a combined sink term of 0.35 Tg yr^{-1} ($0.27\text{ Tg yr}^{-1} + 0.3\text{ Tg}/3.9\text{ yr}$). For the $400\text{--}760\text{ m}$ depth interval, Pack et al. (2015) previously noted a three-orders-of-magnitude discrepancy between the integrated oxidation sink ($0.04\text{--}0.26\text{ Tg yr}^{-1}$) and a benthic source term ($0.024\text{--}0.18\text{ Gg yr}^{-1}$) based on estimates of benthic methane fluxes in the region (Sansone et al. 2004). Although large uncertainties are associated with the estimate of the inventory and the extrapolation of rate constants, our results support the conclusion that much stronger methane sources must exist in the ETNP OMZ (Pack et al. 2015). Whereas the benthic fluxes used in the previous estimate are supported by recent direct measurements on the Mexican margin (Chronopoulou et al. 2017), the integrated benthic flux can be revised upwards by a factor of 3 to $0.07\text{--}0.52\text{ Gg yr}^{-1}$ by expansion of the OMZ core-contacted sediment area from $17,800$ to $51,000\text{ km}^2$ corresponding to a depth interval of $206\text{--}800\text{ m}$ between 8°N and 20°N (Helly and Levin 2004). Yet, even a benthic methane flux of 0.52 Gg yr^{-1} is 670-fold less than the combined loss from oxidation and mixing, and 150-fold less than the loss by mixing alone. It thus seems unrealistic that benthic fluxes required to balance the sinks can be delivered by diffusion from normal marine sediments. Instead, phenomena such as massive venting or very extensive seepage of methane must be involved if the methane pool of the ETNP OMZ originates in the seafloor, though areas with such characteristics have not yet been described in the region.

As an alternative to a benthic source, methane could be produced in the water column as previously suggested (Sansone et al. 2001) and supported by the detection of transcriptionally active methanogenic archaea at anoxic depths in the OMZ (Padilla et al. 2016). Concomitant production and oxidation of methane has been observed in marine surface sediment, where the production is based on C_1 compounds that are not utilized by the otherwise dominating sulfate reducing bacteria (Xiao et al. 2017, 2018). Although methylotrophic methanogens in OMZ waters should face strong competition from nitrate/nitrite-respiring methylotrophs (Beck et al. 2014), they could potentially be active in nitrate and nitrite-depleted microniches, e.g., inside organic-rich aggregates (Bianchi et al. 2018). Thus, both pelagic and benthic origins must be considered in the sleuthing for the source of methane in the ETNP OMZ.

In summary, our results indicate that the ETNP OMZ is not a passive conduit for methane but rather a zone of active methane cycling. Methane oxidation occurs anaerobically and is coupled to nitrate reduction and denitrification, with kinetics that do not appear substantially slower than those observed in oxic waters. Relatives of "*Ca. Methylomirabilis sp.*" of the NC10 clade are the most well-documented anaerobic methane oxidizers in the ETNP OMZ, but their contribution to methane oxidation has yet to be quantified. Potential competitors

include nitrate-reducing ANME-2d archaea related to “*Ca. Methanoperedens*” for which we report preliminary evidence. In addition, the potential role of gammaproteobacterial methanotrophs requires further exploration although a capability for anaerobic methane oxidation has yet to be documented. Another open question pertains to the great imbalance between the estimated sources and sinks for methane with loss by both oxidation and mixing far exceeding benthic diffusive fluxes. In any case, our results suggest that anaerobic methane oxidation attenuates the flux of methane from the anoxic OMZ core substantially. It thus appears that the process will influence methane emissions in the upwelling areas of the ETNP OMZ. Whether anaerobic microbes play a similar role in methane cycling in other OMZs remains to be investigated.

References

- Anantharaman, K., and others. 2018. Expanded diversity of microbial groups that shape the dissimilatory sulfur cycle. *ISME J.* **12**: 1715–1728. doi:10.1038/s41396-018-0078-0.
- Babbin, A. R., R. G. Keil, A. H. Devol, and B. B. Ward. 2014. Organic matter stoichiometry, flux, and oxygen control nitrogen loss in the ocean. *Science* **344**: 406–408. doi:10.1126/science.1248364.
- Beck, D. A. C., and others. 2014. The expanded diversity of methylphilaceae from Lake Washington through cultivation and genomic sequencing of novel ecotypes. *PLoS One* **9**: e102458. doi:10.1371/journal.pone.0102458.
- Becraft, E. D., and others. 2017. Rokubacteria: Genomic giants among the uncultured bacterial phyla. *Front. Microbiol.* **8**: 12. doi:10.3389/fmicb.2017.02264.
- Bédard, C., and R. Knowles. 1989. Physiology, biochemistry, and specific inhibitors of CH₄, NH₄⁺, and CO oxidation by methanotrophs and nitrifiers. *Microbiol. Rev.* **53**: 68–84.
- Berger, S., J. Frank, P. Dalcin Martins, M. S. M. Jetten, and C. U. Welte. 2017. High-quality draft genome sequence of “*Candidatus Methanoperedens* sp.” strain BLZ2, a nitrate-reducing anaerobic methane-oxidizing archaeon enriched in an anoxic bioreactor. *Genome Announc.* **5**: e01159–17. doi:10.1128/genomeA.01159-17.
- Bianchi, D., T. S. Weber, R. Kiko, and C. Deutsch. 2018. Global niche of marine anaerobic metabolisms expanded by particle microenvironments. *Nat. Geosci.* **11**: 263–268. doi:10.1038/s41561-018-0081-0.
- Blees, J., H. Niemann, C. B. Wenk, J. Zopfi, C. J. Schubert, J. S. Jenzer, M. Veronesi, and M. F. Lehmann. 2014. Bacterial methanotrophs drive the formation of a seasonal anoxic benthic nepheloid layer in an alpine lake. *Limnol. Oceanogr.* **59**: 1410–1420. doi:10.4319/lo.2014.59.4.1410.
- Burke, R. A., D. F. Reid, J. M. Brooks, and D. M. Lavoie. 1983. Upper water column methane geochemistry in the eastern tropical North Pacific. *Limnol. Oceanogr.* **28**: 19–32. doi:10.4319/lo.1983.28.1.0019.
- Bussmann, I., A. Matousu, R. Osudar, and S. Mau. 2015. Assessment of the radio ³H-CH₄ tracer technique to measure aerobic methane oxidation in the water column. *Limnol. Oceanogr.: Methods* **13**: 312–327. doi:10.1002/lom3.10027.
- Callahan, B. J., P. J. McMurdie, M. J. Rosen, A. W. Han, A. J. A. Johnson, and S. P. Holmes. 2016. DADA2: High-resolution sample inference from Illumina amplicon data. *Nat. Methods* **13**: 581–583. doi:10.1038/nmeth.3869.
- Caporaso, J. G., C. L. Lauber, W. A. Walters, D. Berg-Lyons, C. A. Lozupone, P. J. Turnbaugh, N. Fierer, and R. Knight. 2011. Global patterns of 16S rRNA diversity at a depth of millions of sequences per sample. *Proc. Natl. Acad. Sci. USA* **108**: 4516–4522. doi:10.1073/pnas.1000080107.
- Chronopoulou, P. M., F. Shelley, W. J. Pritchard, S. T. Maanoja, and M. Trimmer. 2017. Origin and fate of methane in the eastern tropical North Pacific oxygen minimum zone. *ISME J.* **11**: 1386–1399. doi:10.1038/ismej.2017.6.
- Dalsgaard, T., F. J. Stewart, B. Thamdrup, L. De Brabandere, N. P. Revsbech, O. Ulloa, D. E. Canfield, and E. F. DeLong. 2014. Oxygen at nanomolar levels reversibly suppresses process rates and gene expression of anammox and denitrification in the oxygen minimum zone off northern Chile. *MBio* **5**: e01966. doi:10.1128/mBio.01966-14.
- Dam, B., S. Dam, J. Blom, and W. Liesack. 2013. Genome analysis coupled with physiological studies reveals a diverse nitrogen metabolism in *Methylocystis* sp. strain SC2. *PLoS One* **8**: e74767. doi:10.1371/journal.pone.0074767.
- De Brabandere, L., B. Thamdrup, N. P. Revsbech, and R. Foadi. 2012. A critical assessment of the occurrence and extend of oxygen contamination during anaerobic incubations utilizing commercially available vials. *J. Microbiol. Methods* **88**: 147–154. doi:10.1016/j.mimet.2011.11.001.
- De Brabandere, L., D. E. Canfield, T. Dalsgaard, G. E. Friederich, N. P. Revsbech, O. Ulloa, and B. Thamdrup. 2014. Vertical partitioning of nitrogen-loss processes across the oxic-anoxic interface of an oceanic oxygen minimum zone. *Environ. Microbiol.* **16**: 3041–3054. doi:10.1111/1462-2920.12255.
- DeVries, T., C. Deutsch, F. Primeau, B. Chang, and A. Devol. 2012. Global rates of water-column denitrification derived from nitrogen gas measurements. *Nat. Geosci.* **5**: 547–550. doi:10.1038/ngeo1515.
- Ettwig, K. F., T. van Alen, K. T. van de Pas-Schoonen, M. S. M. Jetten, and M. Strous. 2009. Enrichment and molecular detection of denitrifying methanotrophic bacteria of the NC10 phylum. *Appl. Environ. Microbiol.* **75**: 3656–3662. doi:10.1128/AEM.00067-09.
- Ettwig, K. F., and others. 2010. Nitrite-driven anaerobic methane oxidation by oxygenic bacteria. *Nature* **464**: 543–548. doi:10.1038/nature08883.
- Fuchsman, C. A., A. H. Devol, J. K. Sauters, C. McKay, and G. Rocap. 2017. Niche partitioning of the N cycling microbial community of an offshore oxygen deficient zone. *Front. Microbiol.* **8**: 2384. doi:10.3389/fmicb.2017.02384.

- Ganesh, S., D. J. Parris, E. F. De Long, and F. J. Stewart. 2014. Metagenomic analysis of size-fractionated picoplankton in a marine oxygen minimum zone. *ISME J.* **8**: 187–211. doi:[10.1038/ismej.2013.144](https://doi.org/10.1038/ismej.2013.144).
- Ganesh, S., L. A. Bristow, M. Larsen, N. Sarode, B. Thamdrup, and F. J. Stewart. 2015. Size-fraction partitioning of community gene transcription and nitrogen metabolism in a marine oxygen minimum zone. *ISME J.* **9**: 2682–2696. doi:[10.1038/ismej.2015.44](https://doi.org/10.1038/ismej.2015.44).
- Ganesh, S., and others. 2018. Single cell genomic and transcriptomic evidence for the use of alternative nitrogen substrates by anammox bacteria. *ISME J.* **12**: 2706–2722. doi:[10.1038/s41396-018-0223-9](https://doi.org/10.1038/s41396-018-0223-9).
- Garcia, H. E., and L. I. Gordon. 1992. Oxygen solubility in seawater - better fitting equations. *Limnol. Oceanogr.* **37**: 1307–1312. doi:[10.4319/lo.1992.37.6.1307](https://doi.org/10.4319/lo.1992.37.6.1307).
- Garcia-Robledo, E., S. Borisov, I. Klimant, and N. P. Revsbech. 2016. Determination of respiration rates in water with sub-micromolar oxygen concentrations. *Front. Mar. Sci.* **3**: 244. doi:[10.3389/fmars.2016.00244](https://doi.org/10.3389/fmars.2016.00244).
- Garcia-Robledo, E., C. C. Padilla, M. Aldunate, F. J. Stewart, O. Ulloa, A. Paulmier, G. Gregori, and N. P. Revsbech. 2017. Cryptic oxygen cycling in anoxic marine zones. *Proc. Natl. Acad. Sci. USA* **114**: 8319–8324. doi:[10.1073/pnas.1619844114](https://doi.org/10.1073/pnas.1619844114).
- Graf, J. S., and others. 2018. Bloom of a denitrifying methanotroph, '*Candidatus* Methylomirabilis limnetica', in a deep stratified lake. *Environ. Microbiol.* **20**: 2598–2614. doi:[10.1111/1462-2920.14285](https://doi.org/10.1111/1462-2920.14285).
- Grasshoff, K. 1983. Determination of nitrite, p. 139–142. In K. Grasshoff, M. Ehrhardt, and K. Kremling [eds.], *Methods of seawater analysis*. Verlag Chemie.
- Haroon, M. F., S. Hu, Y. Shi, M. Imelfort, J. Keller, P. Hugenholtz, Z. Yuan, and G. W. Tyson. 2013. Anaerobic oxidation of methane coupled to nitrate reduction in a novel archaeal lineage. *Nature* **501**: 567–570. doi:[10.1038/nature12619](https://doi.org/10.1038/nature12619).
- Heintz, M. B., S. Mau, and D. L. Valentine. 2012. Physical control on methanotrophic potential in waters of the Santa Monica Basin, Southern California. *Limnol. Oceanogr.* **57**: 420–432. doi:[10.4319/lo.2012.57.2.0420](https://doi.org/10.4319/lo.2012.57.2.0420).
- Helly, J. J., and L. A. Levin. 2004. Global distribution of naturally occurring marine hypoxia on continental margins. *Deep-Sea Res. Part I Oceanogr. Res. Pap.* **51**: 1159–1168. doi:[10.1016/j.dsr.2004.03.009](https://doi.org/10.1016/j.dsr.2004.03.009).
- Holmes, R. M., A. Aminot, R. Kerouel, B. A. Hooker, and B. J. Peterson. 1999. A simple and precise method for measuring ammonium in marine and freshwater ecosystems. *Can. J. Fish. Aquat. Sci.* **56**: 1801–1808. doi:[10.1139/f99-128](https://doi.org/10.1139/f99-128).
- Hyman, M. R., and P. M. Wood. 1983. Methane oxidation by *Nitrosomonas europaea*. *Biochem. J.* **212**: 31–37. doi:[10.1042/bj2120031](https://doi.org/10.1042/bj2120031).
- Hyman, M. R., I. B. Murton, and D. J. Arp. 1988. Interaction of ammonia monooxygenase from *Nitrosomonas europaea* with alkanes, alkenes, and alkynes. *Appl. Environ. Microbiol.* **54**: 3187–3190.
- Kartal, B., and others. 2011. Molecular mechanism of anaerobic ammonium oxidation. *Nature* **479**: 127–130. doi:[10.1038/nature10453](https://doi.org/10.1038/nature10453).
- Kits, K. D., M. G. Klotz, and L. Y. Stein. 2015. Methane oxidation coupled to nitrate reduction under hypoxia by the Gammaproteobacterium *Methylomonas denitrificans*, sp. nov. type strain FJG1. *Environ. Microbiol.* **17**: 3219–3232. doi:[10.1111/1462-2920.12772](https://doi.org/10.1111/1462-2920.12772).
- Knittel, K., and A. Boetius. 2009. Anaerobic oxidation of methane: Progress with an unknown process. *Annu. Rev. Microbiol.* **63**: 311–334. doi:[10.1146/annurev.micro.61.080706.093130](https://doi.org/10.1146/annurev.micro.61.080706.093130).
- Kozich, J. J., S. L. Westcott, N. T. Baxter, S. K. Highlander, and P. D. Schloss. 2013. Development of a dual-index sequencing strategy and curation pipeline for analyzing amplicon sequence data on the MiSeq Illumina sequencing platform. *Appl. Environ. Microbiol.* **79**: 5112–5120. doi:[10.1128/AEM.01043-13](https://doi.org/10.1128/AEM.01043-13).
- Martens-Habbena, W., and others. 2015. The production of nitric oxide by marine ammonia-oxidizing archaea and inhibition of archaeal ammonia oxidation by a nitric oxide scavenger. *Environ. Microbiol.* **17**: 2261–2274. doi:[10.1111/1462-2920.12677](https://doi.org/10.1111/1462-2920.12677).
- Mau, S., J. Blees, E. Helmke, H. Niemann, and E. Damm. 2013. Vertical distribution of methane oxidation and methanotrophic response to elevated methane concentrations in stratified waters of the Arctic fjord Storfjorden (Svalbard, Norway). *Biogeosciences* **10**: 6267–6278. doi:[10.5194/bg-10-6267-2013](https://doi.org/10.5194/bg-10-6267-2013).
- Naqvi, S. W. A., H. W. Bange, L. Farias, P. M. S. Monteiro, M. I. Scranton, and J. Zhang. 2010. Marine hypoxia/anoxia as a source of CH₄ and N₂O. *Biogeosciences* **7**: 2159–2190. doi:[10.5194/bg-7-2159-2010](https://doi.org/10.5194/bg-7-2159-2010).
- Oswald, K., J. Milucka, A. Brand, S. Littmann, B. Wehrli, M. M. Kuypers, and C. J. Schubert. 2015. Light-dependent aerobic methane oxidation reduces methane emissions from seasonally stratified lakes. *PLoS One* **10**: 22. doi:[10.1371/journal.pone.0132574](https://doi.org/10.1371/journal.pone.0132574).
- Oswald, K., J. Milucka, A. Brand, P. Hach, S. Littmann, B. Wehrli, M. M. M. Kuypers, and C. J. Schubert. 2016. Aerobic gammaproteobacterial methanotrophs mitigate methane emissions from oxic and anoxic lake waters. *Limnol. Oceanogr.* **61**: S101–S118. doi:[10.1002/lno.10312](https://doi.org/10.1002/lno.10312).
- Owens, N. J. P., C. S. Law, R. F. C. Mantoura, P. H. Burkill, and C. A. Llewellyn. 1991. Methane flux to the atmosphere from the Arabian Sea. *Nature* **354**: 293–296. doi:[10.1038/354293a0](https://doi.org/10.1038/354293a0).
- Pack, M. A., M. B. Heintz, W. S. Reeburgh, S. E. Trumbore, D. L. Valentine, X. Xu, and E. R. M. Druffel. 2015. Methane oxidation in the eastern tropical North Pacific Ocean water column. *J. Geophys. Res. Biogeosci.* **120**: 1078–1092. doi:[10.1002/2014JG002900](https://doi.org/10.1002/2014JG002900).

- Padilla, C. C., and others. 2016. NC10 bacteria in marine oxygen minimum zones. *ISME J.* **10**: 2067–2071. doi:10.1038/ismej.2015.262.
- Padilla, C. C., A. D. Bertagnolli, L. A. Bristow, N. Sarode, J. B. Glass, B. Thamdrup, and F. J. Stewart. 2017. Metagenomic binning recovers a transcriptionally active gammaproteobacterium linking methanotrophy to partial denitrification in an anoxic oxygen minimum zone. *Front. Mar. Sci.* **4**: 23. doi:10.3389/fmars.2017.00023.
- Paulmier, A., and D. Ruiz-Pino. 2009. Oxygen minimum zones (OMZs) in the modern ocean. *Prog. Oceanogr.* **80**: 113–128. doi:10.1016/j.pocean.2008.08.001.
- Pruitt, K. D., T. Tatusova, and D. R. Maglott. 2007. NCBI reference sequences (RefSeq): A curated non-redundant sequence database of genomes, transcripts and proteins. *Nucleic Acids Res.* **35**: D61–D65. doi:10.1093/nar/gkl842.
- Raghoebarsing, A. A., and others. 2006. A microbial consortium couples anaerobic methane oxidation to denitrification. *Nature* **440**: 918–921. doi:10.1038/nature04617.
- Reeburgh, W. S. 2007. Oceanic methane biogeochemistry. *Chem. Rev.* **107**: 486–513. doi:10.1021/cr050362v.
- Reeburgh, W. S., B. B. Ward, S. C. Whalen, K. A. Sandbeck, K. A. Kilpatrick, and L. J. Kerkhof. 1991. Black-Sea methane geochemistry. *Deep-Sea Res. Part A Oceanogr. Res. Pap.* **38**: S1189–S1210. doi:10.1016/S0198-0149(10)80030-5.
- Revsbech, N. P., L. H. Larsen, J. Gundersen, T. Dalsgaard, O. Ulloa, and B. Thamdrup. 2009. Determination of ultra-low oxygen concentrations in oxygen minimum zones by the STOX sensor. *Limnol. Oceanogr.: Methods* **7**: 371–381. doi:10.4319/lom.2009.7.371.
- Sansone, F. J., B. N. Popp, A. Gasc, A. W. Graham, and T. M. Rust. 2001. Highly elevated methane in the eastern tropical North Pacific and associated isotopically enriched fluxes to the atmosphere. *Geophys. Res. Lett.* **28**: 4567–4570. doi:10.1029/2001GL013460.
- Sansone, F. J., A. W. Graham, and W. M. Berelson. 2004. Methane along the Mexican margin. *Limnol. Oceanogr.* **49**: 2242–2255. doi:10.4319/lo.2004.49.6.2242.
- Schmieder, R., Y. W. Lim, and R. Edwards. 2012. Identification and removal of ribosomal RNA sequences from metatranscriptomes. *Bioinformatics* **28**: 433–435. doi:10.1093/bioinformatics/btr669.
- Steinle, L., and others. 2015. Water column methanotrophy controlled by a rapid oceanographic switch. *Nat. Geosci.* **8**: 378–382. doi:10.1038/ngeo2420.
- Steinle, L., and others. 2017. Effects of low oxygen concentrations on aerobic methane oxidation in seasonally hypoxic coastal waters. *Biogeosciences* **14**: 1631–1645. doi:10.5194/bg-14-1631-2017.
- Tavormina, P. L., W. Ussler, J. A. Steele, S. A. Connon, M. G. Klotz, and V. J. Orphan. 2013. Abundance and distribution of diverse membrane-bound monooxygenase (Cu-MMO) genes within the Costa Rica oxygen minimum zone. *Environ. Microbiol. Rep.* **5**: 414–423. doi:10.1111/1758-2229.12025.
- Thamdrup, B., T. Dalsgaard, N. P. Revsbech. 2012. Widespread functional anoxia in the oxygen minimum zone of the Eastern South Pacific. *Deep-Sea Res. Part I Oceanogr. Res. Pap.* **65**: 36–45. doi:10.1016/j.dsr.2012.03.001.
- Thamdrup, B., T. Dalsgaard, M. M. Jensen, O. Ulloa, L. Farias, and R. Escibano. 2006. Anaerobic ammonium oxidation in the oxygen-deficient waters off northern Chile. *Limnol. Oceanogr.* **51**: 2145–2156. doi:10.4319/lo.2006.51.5.2145.
- Tiano, L., E. Garcia-Robledo, T. Dalsgaard, A. H. Devol, B. B. Ward, O. Ulloa, D. E. Canfield, and N. P. Revsbech. 2014. Oxygen distribution and aerobic respiration in the north and south eastern tropical Pacific oxygen minimum zones. *Deep-Sea Res. Part I Oceanogr. Res. Pap.* **94**: 173–183. doi:10.1016/j.dsr.2014.10.001.
- Valentine, D. L., D. C. Blanton, W. S. Reeburgh, and M. Kastner. 2001. Water column methane oxidation adjacent to an area of active hydrate dissociation, Eel River Basin. *Geochim. Cosmochim. Acta* **65**: 2633–2640. doi:10.1016/S0016-7037(01)00625-1.
- Ward, B. B., K. A. Kilpatrick, P. C. Novelli, and M. I. Scranton. 1987. Methane oxidation and methane fluxes in the ocean surface-layer and deep anoxic waters. *Nature* **327**: 226–229. doi:10.1038/327226a0.
- Wiesenburg, D. A., and N. L. Guinasso Jr. 1979. Equilibrium solubilities of methane, carbon monoxide, and hydrogen in water and sea water. *J. Chem. Eng. Data* **24**: 356–360. doi:10.1021/je60083a006.
- Xiao, K. Q., F. Beulig, K. U. Kjeldsen, B. B. Jørgensen, and N. Risgaard-Petersen. 2017. Concurrent methane production and oxidation in surface sediment from Aarhus Bay, Denmark. *Front. Microbiol.* **8**: 12. doi:10.3389/fmicb.2017.01198.
- Xiao, K. Q., F. Beulig, H. Roy, B. B. Jørgensen, and N. Risgaard-Petersen. 2018. Methylophilic methanogenesis fuels cryptic methane cycling in marine surface sediment. *Limnol. Oceanogr.* **63**: 1519–1527. doi:10.1002/lno.10788.

Acknowledgments

We are grateful to Andrew Burns for help in sequencing analysis, Michael W. Hansen for methane analysis, the scientific party of cruise OC1710 for help with sample collection, and the captain and crew of the R/V *Oceanus* for enabling sample collection. This work was supported by the European Research Council (ERC Advanced Grant 695599 NOVAMOX to BT) and the National Science Foundation (1151698, 1558916, and 1564559 to FJS).

Conflict of Interest

None declared.

Submitted 14 November 2018

Revised 21 March 2019

Accepted 15 May 2019

Associate editor: Leila Hamdan